

Connecting the Popularity Adjusted Block Model to the Generalized Random Dot Product Graph for Community Detection and Parameter Estimation

Abstract

We connect two random graph models, the Popularity Adjusted Block Model (PABM) and the Generalized Random Dot Product Graph (GRDPG), demonstrating that a PABM is a GRDPG in which communities correspond to certain mutually orthogonal subspaces of latent positions. This insight leads to the construction of improved algorithms for community detection and parameter estimation with PABM. Using established asymptotic properties of Adjacency Spectral Embedding (ASE) for GRDPG, we derive asymptotic properties of these algorithms, including algorithms that rely on Sparse Subspace Clustering (SSC). We illustrate these properties via simulation.

1 Introduction

Statistical analysis on graphs or networks often involves the partitioning of a graph into disconnected subgraphs or clusters. This is often motivated by the assumption that there exist underlying and unobserved communities to which each vertex of the graph belongs, and edges between pairs of vertices are determined by drawing from a probability distribution based on the community relationships between each pair. The goal of this analysis then is population community detection, or the recovery of the true underlying community labels for each vertex, up to permutation, with some additional parameter estimation being of possible interest, assuming some underlying probability model. One such model is the Stochastic Block Model (SBM), first proposed by Lorrain and White [9], which assumes that the edge probability from one vertex to another follows a Bernoulli distribution with fixed probabilities for each pair of community labels. Other random graph models have been proposed and studied, such as the Degree-Corrected Block Model (DCBM), introduced by Karrer and Newman [7], which is a generalization of the SBM. The Popularity Adjusted Block Model (PABM) was then introduced by Sengupta and Chen [15] as a generalization of the DCBM to address the heterogeneity of edge probabilities within and between communities while still maintaining distinct community structure.

The underlying similarity among the SBM, PABM, and other such models is that they involve a symmetric edge probability matrix $P \in [0, 1]^{n \times n}$ where n is the number of vertices in the graph. An undirected and unweighted graph is then drawn from this edge probability matrix such that the existence of an edge between each pair of vertices i and j is given by $\text{Bernoulli}(P_{ij})$. For example, for the SBM with two communities for which the within-community edge probability is ξ and the between-community edge probability is η , the entries of P consist of $P_{ij} = \xi$ if i and j are in the same community and $i \neq j$, $P_{ij} = \eta$ if i and j belong to separate communities, and $P_{ii} = 0$.

The Random Dot Product Graph (RDPG) model proposed by Young and Scheinerman [20] is another graph model with Bernoulli edge probabilities. Under this model, each vertex of the graph can be represented by a point in some latent space such that the edge probability

between any pair of vertices is given by their corresponding dot product in the latent space, i.e., given a latent positions $x_1, \dots, x_n \in \mathbb{R}^d$, the edge probability matrix is $P = XX^\top$ where $X = \begin{bmatrix} x_1 & \dots & x_n \end{bmatrix}^\top$. The assortative SBM is equivalent to a special case of the RDPG for which all vertices of a given community share the same position in the latent space [10]. It has also been shown that similar random graph models, including the DCBM, can be represented in a similar fashion [10, 14]. An analogous property exists for the PABM, not for the RDPG model but the *Generalized* Random Dot Product Graph (GRDPG) model, which is an extension of the RDPG to allow edge probability matrices that are not positive semidefinite. This relationship will be explored in this paper and exploited to construct algorithms for community detection and parameter estimation for the PABM.

1.1 Notation and Scope

Let $G = (V, E)$ be an unweighted, undirected, and hollow graph with vertex set V ($|V| = n$) and edge set E . $A \in \{0, 1\}^{n \times n}$ represents the adjacency matrix of G such that $A_{ij} = 1$ if there exists an edge between vertices i and j and 0 otherwise. Because G is symmetric and hollow, $A_{ij} = A_{ji}$ and $A_{ii} = 0$ for each $i, j \in [n]$. We further restrict our analyses to Bernoulli graphs. Let $P \in [0, 1]^{n \times n}$ be a symmetric matrix of edge probabilities. Graph G is sampled from P by drawing $A_{ij} \stackrel{\text{indep}}{\sim} \text{Bernoulli}(P_{ij})$ for each $1 \leq i < j \leq n$ (setting $A_{ji} = A_{ij}$ and $A_{ii} = 0$). We denote $A \sim \text{BernoulliGraph}(P)$ as graph with adjacency matrix A sampled from edge probability matrix P in this manner. If each vertex has a hidden label in $[K]$, they are denoted as z_1, \dots, z_n . Finally, we denote $X = \begin{bmatrix} x_1 & \dots & x_n \end{bmatrix}^\top \in \mathbb{R}^{n \times d}$ as the collection of n latent vectors $x_1, \dots, x_n \in \mathbb{R}^d$.

2 Connecting the Popularity Adjusted Block Model to the Generalized Random Dot Product Graph

In this section, we show that the PABM is a special case of the GRDPG, i.e., graph G drawn from the PABM can be represented by a collection of latent vectors in Euclidean space. We further show that the latent configuration that induces the PABM consists of

orthogonal subspaces with each subspace corresponding to a community.

2.1 The Popularity Adjusted Block Model and the Generalized Random Dot Product Graph

Definition 1 (Popularity Adjusted Block Model). *Let $P \in [0, 1]^{n \times n}$ be a symmetric edge probability matrix for a graph $G = (V, E)$ with adjacency matrix A such that $A \sim \text{BernoulliGraph}(P)$. Let each vertex have a community label between 1 and K . Then G is drawn from a Popularity Adjusted Block Model if each vertex has K popularity parameters that describe its affinity toward each of the K communities, i.e., vertex i has popularity parameters $\lambda_{i1}, \dots, \lambda_{iK}$, and each $P_{ij} = \lambda_{iz_j} \lambda_{jz_i}$.*

Another characterization of the PABM is as follows. Let the rows and columns of P be arranged by community label such that $n_k \times n_l$ block $P^{(kl)}$ describes the edge probabilities between vertices in communities k and l ($P^{(lk)} = (P^{(kl)})^\top$). If each block $P^{(kl)}$ can be written as the outer product of two vectors:

$$P^{(kl)} = \lambda^{(kl)} (\lambda^{(lk)})^\top \quad (1)$$

for a set of K^2 popularity vectors $\{\lambda^{(st)}\}_{s,t=1}^K$ where each $\lambda^{(st)}$ is a column vector of dimension n_s , then graph G is drawn from a PABM with parameters $\{\lambda^{(st)}\}_K$ if its corresponding adjacency matrix $A \sim \text{BernoulliGraph}(P)$.

We will use the notation $A \sim \text{PABM}(\{\lambda^{(kl)}\}_K)$ to denote a random adjacency matrix A drawn from a PABM with parameters $\lambda^{(kl)}$ consisting of K underlying communities.

Definition 2 (Generalized Random Dot Product Graph). *Let graph $G = (V, E)$ be drawn as $A \sim \text{BernoulliGraph}(P)$. If $\exists X \in \mathbb{R}^{n \times d}$ such that*

$$P = X I_{p,q} X^\top \quad (2)$$

for some $d, p, q \in \mathbb{N}$ and $p + q = d$, then G is drawn from the Generalized Random Dot

Product Graph with latent positions $x_1, \dots, x_n \in \mathbb{R}^d$ and signature (p, q) .

We will use the notation $A \sim \text{GRDPG}_{p,q}(X)$ to denote a random adjacency matrix A drawn from latent positions X and signature (p, q) . If instead of fixed latent positions, they are drawn $X_1, \dots, X_n \stackrel{\text{iid}}{\sim} F$, we denote the GRDPG as $(A, X) \sim \text{GRDPG}_{p,q}(F, n)$.

Definition 3 (Indefinite Orthogonal Group). *The indefinite orthogonal group with signature (p, q) is the set $\{Q \in \mathbb{R}^{d \times d} : QI_{p,q}Q^\top = I_{p,q}\}$, denoted as $\mathbb{O}(p, q)$.*

Remark. Like the RDPG, the latent positions of a GRDPG are not unique [13]. More specifically, if $P_{ij} = x_i^\top I_{p,q} x_j$, then we also have for any $Q \in \mathbb{O}(p, q)$, $(Qx_i)^\top I_{p,q} (Qx_j) = x_i^\top (Q^\top I_{p,q} Q) x_j = x_i^\top I_{p,q} x_j = P_{ij}$. Unlike in the RDPG case, transforming the latent positions via multiplication by $Q \in \mathbb{O}(p, q)$ does not necessarily maintain interpoint angles or distances.

2.2 Connecting the PABM to the GRDPG

Theorem 1 (Connecting the PABM to the GRDPG for $K = 2$). *Let*

$$X = \begin{bmatrix} \lambda^{(11)} & \lambda^{(12)} & 0 & 0 \\ 0 & 0 & \lambda^{(21)} & \lambda^{(22)} \end{bmatrix} \quad \text{and} \quad U = \begin{bmatrix} 1 & 0 & 0 & 0 \\ 0 & 0 & 1/\sqrt{2} & 1/\sqrt{2} \\ 0 & 0 & 1/\sqrt{2} & -1/\sqrt{2} \\ 0 & 1 & 0 & 0 \end{bmatrix},$$

where the $\{\lambda^{(kl)}\}$ are as defined in Definition 1. Then $A \sim \text{GRDPG}_{3,1}(XU)$ and $B \sim \text{PABM}(\{(\lambda^{(kl)})\})$ are identically distributed.

Theorem 2 (Generalization to $K > 2$). *There exists a block diagonal matrix $X \in \mathbb{R}^{n \times K^2}$ defined by PABM parameters $\{\lambda^{(kl)}\}_K$ and orthonormal matrix $U \in \mathbb{R}^{K^2 \times K^2}$ that is fixed for each K such that $A \sim \text{GRDPG}_{K(K+1)/2, K(K-1)/2}(XU)$ and $A \sim \text{PABM}(\{(\lambda^{(kl)})\}_K)$ are equivalent.*

Proof. First define the following matrices from $\{\lambda^{(kl)}\}_K$:

$$\Lambda^{(k)} = \left[\lambda^{(k,1)} \mid \dots \mid \lambda^{(k,K)} \right] \in \mathbb{R}^{n_k \times K}, \quad X = \text{blockdiag}(\Lambda^{(1)}, \dots, \Lambda^{(K)}) \in \mathbb{R}^{n \times K^2} \quad (3)$$

$$L^{(k)} = \text{blockdiag}(\lambda^{(1k)}, \dots, \lambda^{(Kk)}) \in \mathbb{R}^{n \times K}, \quad Y = \left[L^{(1)} \mid \dots \mid L^{(K)} \right] \in \mathbb{R}^{n \times K^2}. \quad (4)$$

We then have $P = XY^\top$. Similar to the $K = 2$ case, we have $Y = X\Pi$ for a permutation matrix Π , resulting in $P = X\Pi X^\top$. The permutation described by Π has K fixed points, which correspond to K eigenvalues equal to 1 with corresponding eigenvectors e_k where $k = r(K+1) + 1$ for $r = 0, \dots, K-1$. It also has $\binom{K}{2} = K(K-1)/2$ cycles of order 2. Each cycle corresponds to a pair of eigenvalues $+1$ and -1 and a pair of eigenvectors $(e_s + e_t)/\sqrt{2}$ and $(e_s - e_t)/\sqrt{2}$.

Then Π has $p = K(K+1)/2$ eigenvalues equal to 1 and $q = K(K-1)/2$ eigenvalues equal to -1 . We therefore have

$$\Pi = UI_{K(K+1)/2, K(K-1)/2} U^\top \quad (5)$$

where U is a $K^2 \times K^2$ orthogonal matrix. The edge probability matrix can then be written as

$$P = XU I_{p,q}(XU)^\top \quad (6)$$

We can therefore describe the PABM with K communities as a GRDPG with latent positions XU and signature $(p, q) = (\frac{1}{2}K(K+1), \frac{1}{2}K(K-1))$. \square

Example ($K = 3$). Using the same notation as in Theorem 2, we can define

$$X = \begin{bmatrix} \lambda^{(11)} & \lambda^{(12)} & \lambda^{(13)} & 0 & 0 & 0 & 0 & 0 & 0 \\ 0 & 0 & 0 & \lambda^{(21)} & \lambda^{(22)} & \lambda^{(23)} & 0 & 0 & 0 \\ 0 & 0 & 0 & 0 & 0 & 0 & \lambda^{(31)} & \lambda^{(32)} & \lambda^{(33)} \end{bmatrix},$$

$$Y = \begin{bmatrix} \lambda^{(11)} & 0 & 0 & \lambda^{(12)} & 0 & 0 & \lambda^{(13)} & 0 & 0 \\ 0 & \lambda^{(21)} & 0 & 0 & \lambda^{(22)} & 0 & 0 & \lambda^{(23)} & 0 \\ 0 & 0 & \lambda^{(31)} & 0 & 0 & \lambda^{(32)} & 0 & 0 & \lambda^{(33)} \end{bmatrix}.$$

Then $Y = X\Pi$ and $P = XY^\top$ where Π is a permutation matrix of the form

$$\Pi = \begin{bmatrix} 1 & 0 & 0 & 0 & 0 & 0 & 0 & 0 & 0 \\ 0 & 0 & 0 & 1 & 0 & 0 & 0 & 0 & 0 \\ 0 & 0 & 0 & 0 & 0 & 0 & 1 & 0 & 0 \\ 0 & 1 & 0 & 0 & 0 & 0 & 0 & 0 & 0 \\ 0 & 0 & 0 & 0 & 1 & 0 & 0 & 0 & 0 \\ 0 & 0 & 0 & 0 & 0 & 0 & 0 & 1 & 0 \\ 0 & 0 & 1 & 0 & 0 & 0 & 0 & 0 & 0 \\ 0 & 0 & 0 & 0 & 0 & 1 & 0 & 0 & 0 \\ 0 & 0 & 0 & 0 & 0 & 0 & 0 & 0 & 1 \end{bmatrix}.$$

The matrix Π corresponds to a permutation of $\{1, 2, \dots, 9\}$ with the following decomposition.

1. Positions 1, 5, 9 are fixed.
2. There are three cycles of length 2, namely (2, 4), (3, 7), and (6, 8).

We can therefore write Π as $\Pi = UI_{6,3}U^\top$ where the first three columns of U consist of e_1 , e_5 , and e_9 corresponding to the fixed positions 1, 5, and 9, the next three columns consist of eigenvectors $(e_k + e_l)/\sqrt{2}$, and the last three columns consist of eigenvectors $(e_k - e_l)/\sqrt{2}$, where pairs (k, l) correspond to the cycles of order 2 described above.

The matrix P can then be written as a generalized random dot product graph where the latent positions are the rows of the matrix

$$XU = \begin{bmatrix} \lambda^{(11)} & 0 & 0 & \lambda^{(12)}/\sqrt{2} & \lambda^{(13)}/\sqrt{2} & 0 & \lambda^{(12)}/\sqrt{2} & \lambda^{(13)}/\sqrt{2} & 0 \\ 0 & \lambda^{(22)} & 0 & \lambda^{(21)}/\sqrt{2} & 0 & \lambda^{(23)}/\sqrt{2} & -\lambda^{(21)}/\sqrt{2} & 0 & \lambda^{(23)}/\sqrt{2} \\ 0 & 0 & \lambda^{(33)} & 0 & \lambda^{(31)}/\sqrt{2} & \lambda^{(32)}/\sqrt{2} & 0 & -\lambda^{(31)}/\sqrt{2} & -\lambda^{(32)}/\sqrt{2} \end{bmatrix}$$

3 Methods

Two inference objectives arise from the PABM:

1. Community membership identification (up to permutation).
2. Parameter estimation (estimating $\lambda^{(kl)}$'s).

In our methods, we assume that K , the number of communities, is known beforehand and does not require estimation.

3.1 Related work

Sengupta and Chen, who first proposed the PABM, used Modularity Maximization (MM) and the Extreme Points (EP) algorithm [8] for community detection and parameter estimation. They were able to show that as the sample size increases, the proportion of misclassified community labels (up to permutation) goes to 0.

Noroozi, Rimal, and Pensky [12] used Sparse Subspace Clustering (SSC) for community detection in the PABM. SSC is performed by solving an optimization problem for each observed point. Given $X \in \mathbb{R}^{n \times d}$ with vectors $x_i^\top \in \mathbb{R}^d$ as rows of X , the optimization problem $c_i = \arg \min_c \|c\|_1$ subject to $x_i = Xc$ and $c^{(i)} = 0$ is solved for each $i = 1, \dots, n$. The solutions are collected into matrix $C = \begin{bmatrix} c_1 & \dots & c_n \end{bmatrix}^\top$ to construct an affinity matrix $B = |C| + |C^\top|$. If each x_i lie perfectly on one of K subspaces, B describes an undirected graph consisting of K disjoint subgraphs, i.e., $B_{ij} = 0$ if x_i, x_j are in different subspaces. If X instead represents points near K subspaces with some noise, a final graph partitioning step may be performed (e.g., edge thresholding or spectral clustering).

In practice, SSC is often performed by solving the LASSO problems

$$c_i = \arg \min_c \frac{1}{2} \|x_i - X_{-i}c\|_2^2 + \lambda \|c\|_1 \quad (7)$$

for some sparsity parameter $\lambda > 0$. The c_i vectors are then collected into C and B as before.

Definition 4 (Subspace Detection Property). *Let $X = \begin{bmatrix} x_1 & \dots & x_n \end{bmatrix}^\top$ be noisy points sampled from K subspaces. Let C and B be constructed from the solutions of LASSO problems as described in (7). If each column of C has nonzero norm and $B_{ij} = 0 \forall x_i$ and x_j sampled from different subspaces, then X obeys the subspace detection property.*

Remark. In practice, a noisy sample X often does not obey the subspace detection property. In such cases, B is treated as an affinity matrix for a graph which is then partitioned into

K subgraphs to obtain the clustering. On the other hand, if X does obey the subspace detection property, B describes a graph with at least K disconnected subgraphs. Ideally, when the subspace detection property holds, there are exactly K subgraphs which map to each subspace, but it could be the case that some of the subspaces are represented by multiple disconnected subgraphs. The subspace detection property is contingent on choosing a sufficiently large sparsity parameter λ .

Theorem 2 suggests that SSC is appropriate for community detection for the PABM. More precisely, Theorem 2 says that each community consists of a K -dimensional subspace, and together the subspaces lie in \mathbb{R}^{K^2} . The natural approach then is to perform SSC on the ASE of P or A . Noroozi et al. instead applied SSC to P and A , foregoing embedding altogether.

Using results from Soltanolkotabi and Candés [16], it can be easily shown that the subspace detection property holds for XU , which is an ASE of P . More specifically, if points lie exactly on mutually orthogonal subspaces, then the subspace detection property will hold with probability 1, and this is exactly the case for the PABM (Theorem 2). Much of our work is then built on Rubin-Delanchy et al., who describe the convergence behavior of the ASE of A to the ASE of P , and Wang and Xu [19], who show the necessary conditions for the subspace detection property to hold in noisy cases where the points lie near subspaces.

3.2 Community detection

We previously stated one possible set of latent positions that result in the edge probability matrix of a PABM, $P = (XU)I_{p,q}(XU)^\top$. If we have (or can estimate) XU directly, then both the community detection and parameter identification problem are trivial since U is orthonormal and fixed for each value of K . However, direct identification or estimation of XU is not possible [13].

If we decompose $P = ZI_{p,q}Z^\top$, then $\exists Q \in \mathbb{O}(p, q)$ such that $XU = ZQ$. Even if we start with the exact edge probability matrix, we cannot recover the “original” latent positions XU . Note that unlike in the case of the RDPG, Q is not necessarily an orthogonal matrix. If z_i ’s are the rows of XU , then $\|z_i - z_j\|^2 \neq \|Qz_i - Qz_j\|^2$, and $\langle z_i, z_j \rangle \neq \langle Qz_i, Qz_j \rangle$. This

Algorithm 1: Orthogonal Spectral Clustering.

Data: Adjacency matrix A , number of communities K

Result: Community assignments $1, \dots, K$

- 1 Compute the eigenvectors of A that correspond to the $K(K+1)/2$ most positive eigenvalues and $K(K-1)/2$ most negative eigenvalues. Construct V using these eigenvectors as its columns.
 - 2 Compute $B = |nVV^\top|$, applying $|\cdot|$ entry-wise.
 - 3 Construct graph G using B as its similarity matrix.
 - 4 Partition G into K disconnected subgraphs (e.g., using edge thresholding or spectral clustering).
 - 5 Map each partition to the community labels $1, \dots, K$.
-

prevents us from using the properties of XU directly. In particular, if $Q \in \mathbb{O}(n)$, then we could use the fact that $\langle z_i, z_j \rangle = \langle Qz_i, Qz_j \rangle = 0$ if vertices i and j are in different communities.

The explicit form of XU represents points in \mathbb{R}^{K^2} such that points within each community lie on K -dimensional orthogonal subspaces. Multiplication by $Q \in \mathbb{O}(p, q)$ removes the orthogonality property but retains the property that each community is represented by a K -dimensional subspace. Therefore, the ASE of P results in subspaces that correspond to each community, suggesting the use of SSC. Before exploring SSC, we will first consider a different approach.

Theorem 3. *Let $P = VDV^\top$ be the spectral decomposition of the edge probability matrix. Let $B = nVV^\top$. Then $B_{ij} = 0$ if vertices i and j are from different communities.*

Theorem 3 provides perfect community detection given P . Letting $|B|$ be the affinity matrix for graph G , G is partitioned into at least K disjoint subgraphs since each of the K communities have no edges between them. Similar to the subspace detection property, it could be the case that some of the communities are represented by multiple disjoint subgraphs in G , in which case additional reconstruction is required to identify the communities exactly.

Using A instead of P introduces error, which converges to 0 almost surely:

Theorem 4. *Let \hat{B}_n with entries $\hat{B}_n^{(ij)}$ be the affinity matrix from OSC (Alg. 1). Then \forall pairs (i, j) belonging to different communities and sparsity factor satisfying $n\rho_n = \omega\{(\log n)^{4c}\}$,*

$$\max_{i,j} |n(\hat{v}_n^{(i)})^\top \hat{v}_n^{(j)}| = O_P\left(\frac{(\log n)^c}{\sqrt{n\rho_n}}\right) \quad (8)$$

This provides the result that for i, j in different communities, $\hat{B}_n^{(ij)} \xrightarrow{a.s.} 0$.

Theorems 2, 3, and 4 also provide a very natural path toward using SSC for community detection for the PABM. We established in Theorem 2 that an ASE of the edge probability matrix P can be constructed such that the communities lie on mutually orthogonal subspaces, and this property can be recovered from the eigenvectors of P . Then Theorems 3 and 4 show that this property holds for the unscaled ASE of A drawn from P as $n \rightarrow \infty$.

Theorem 5. *Let P_n describe the edge probability matrix of the PABM with n vertices, and let $A_n \sim \text{Bernoulli}(P_n)$. Let \hat{V}_n be the matrix of eigenvectors of A_n corresponding to the $K(K+1)/2$ most positive and $K(K-1)/2$ most negative eigenvalues. Then $\exists \lambda > 0$ and $N \in \mathbb{N}$ such that when $n > N$, $\sqrt{n}\hat{V}_n$ obeys the subspace detection property with probability 1.*

Remark. The proof of Theorem 5 is a direct consequence of Theorem 6 from Wang and Xu and the fact that the unscaled ASE of P_n consists of orthogonal subspaces. Wang and Xu assume that the points in the embedding are all of unit length, and while we apply this normalization in the simulated examples, it is not strictly necessary for Theorem 5 due to orthogonality.

3.3 Parameter estimation

For any edge probability matrix P for the PABM such that the rows and columns are organized by community, the kl^{th} block is an outer product of two vectors, i.e., $P^{(kl)} = \lambda^{(kl)}(\lambda^{(lk)})^\top$. Therefore, given $P^{(kl)}$, $\lambda^{(kl)}$ and $\lambda^{(lk)}$ are solvable up to multiplicative constant

Algorithm 2: Sparse Subspace Clustering using LASSO [19].

Data: Adjacency matrix A , number of communities K , hyperparameter λ

Result: Community assignments $1, \dots, K$

- 1 Find V , the matrix of eigenvectors of A corresponding to the $K(K+1)/2$ most positive and the $K(K-1)/2$ most negative eigenvalues.
 - 2 Normalize $V \leftarrow \sqrt{n}V$.
 - 3 **for** $i = 1, \dots, n$ **do**
 - 4 Assign v_i^\top as the i^{th} row of V . Assign $V_{-i} = \begin{bmatrix} v_1 & \dots & v_{i-1} & v_{i+1} & \dots & v_n \end{bmatrix}^\top$.
 - 5 Solve the LASSO problem $c_i = \arg \min_\beta \frac{1}{2} \|v_i - V_{-i}\beta\|_2^2 + \lambda \|\beta\|_1$.
 - 6 Assign $\tilde{c}_i = \begin{bmatrix} c_i^{(1)} & \dots & c_i^{(i-1)} & 0 & c_i^{(i)} & \dots & c_i^{(n-1)} \end{bmatrix}^\top$ such that the superscript is the index of \tilde{c}_i .
 - 7 **end**
 - 8 Assign $C = \begin{bmatrix} \tilde{c}_1 & \dots & \tilde{c}_n \end{bmatrix}$.
 - 9 Compute the affinity matrix $B = |C| + |C^\top|$.
 - 10 Construct graph G using B as its similarity matrix.
 - 11 Partition G into K disconnected subgraphs (e.g., using edge thresholding or spectral clustering).
 - 12 Map each partition to the community labels $1, \dots, K$.
-

using singular value decomposition. More specifically, let $P^{(kl)} = (\sigma^{(kl)})^2 u^{(kl)} (v^{(kl)})^\top$ be the singular value decomposition of $P^{(kl)}$. $u^{(kl)} \in \mathbb{R}^{n_k}$ and $v^{(kl)} \in \mathbb{R}^{n_l}$ are vectors and $\sigma^{(kl)}$ is a scalar. Then $\lambda^{(kl)} = s_1 u^{(kl)}$ and $\lambda^{(lk)} = s_2 v^{(kl)}$ for unidentifiable $s_1 s_2 = (\sigma^{(kl)})^2$. Given the adjacency matrix A instead of edge probability matrix P , we can simply use plug-in estimators by taking the SVD of each $A^{(kl)}$. Since each $\lambda^{(kl)}$ is not strictly identifiable, we instead estimate each $\tilde{\lambda}^{(kl)} = \sigma^{(kl)} u^{(kl)}$.

Theorem 6. *Under regularity and sparsity assumptions, given fixed K ,*

$$\max_{k,l \in \{1, \dots, K\}} \|\hat{\lambda}^{(kl)} - \lambda^{(kl)}\| = O_P \left(\frac{(\log n_k)^c}{\sqrt{n_k}} \right) \quad (9)$$

Algorithm 3: PABM parameter estimation.

Data: Adjacency matrix A , community assignments $1, \dots, K$

Result: PABM parameter estimates $\{\hat{\lambda}^{(kl)}\}_K$.

- 1 Arrange the rows and columns of A by community such that each $A^{(kl)}$ block consists of estimated edge probabilities between communities k and l .
 - 2 **for** $k, l = 1, \dots, K, k \leq l$ **do**
 - 3 Compute $A^{(kl)} = U\Sigma V^\top$, the SVD of the kl^{th} block.
 - 4 Assign $u^{(kl)}$ and $v^{(kl)}$ as the first columns of U and V . Assign $(\sigma^{(kl)})^2 \leftarrow \Sigma_{11}$.
 - 5 Assign $\hat{\lambda}^{(kl)} \leftarrow \pm\sigma^{(kl)}u^{(kl)}$ and $\hat{\lambda}^{(lk)} \leftarrow \pm\sigma^{(kl)}v^{(kl)}$.
 - 6 **end**
-

4 Simulated Examples

For each simulation, community labels are drawn from a multinomial distribution, the popularity vectors $\{\lambda^{(kl)}\}_K$ are drawn from two types of joint distributions depending on whether $k = l$, the edge probability matrix P is constructed using the popularity vectors, and finally an unweighted and undirected adjacency matrix A is drawn from P . OSC is then used for community detection, and this method is compared against SSC [12, 17] and MM [3] [15]. True community labels are used with Algorithm 3 to estimate the popularity vectors $\{\lambda^{(kl)}\}_K$, and this method is then compared against an MLE-based estimator described by Noroozi et al. and Sengupta and Chen.

Modularity Maximization is NP-hard, so Sengupta and Chen used the Extreme Points (EP) algorithm [8], which is $O(n^{K-1})$, as a greedy relaxation of the optimization problem. For these simulations, the Louvain algorithm was used for modularity maximization, as Sengupta and Chen's implementation proved to be prohibitively computationally expensive for $K > 2$. For $K = 2$, it was verified that the Louvain algorithm produces comparable results to EP-MM.

Two implementations of SSC are shown here. The first method, denoted as SSC-A, treats the columns of the adjacency matrix A as points in \mathbb{R}^n , as described in Noroozi et al..

The second method, denoted as SSC-ASE, first embeds A and then performs SSC on the embedding, as described in algorithm 2. The sparsity parameter λ was chosen via a preliminary cross-validation experiment. For the final clustering step, a Gaussian Mixture Model was fit on the normalized Laplacian eigenmap of the affinity matrix B .

For comparing methods, we define the community detection error as:

$$L_c(\hat{\sigma}, \sigma; \{v_i\}) = \min_{\pi} \sum_i I(\pi \circ \hat{\sigma}(v_i) = \sigma(v_i))$$

where $\sigma(v_i)$ is the true community label of vertex v_i , $\hat{\sigma}(v_i)$ is the predicted label of v_i , and π is a permutation operator. This is effectively the "misclustering count" of clustering function $\hat{\sigma}$.

We also define two types of parameter estimation error. First, we estimate the popularity vectors directly and compute the RMSE. In this case, the "true" popularity vectors are derived from taking the SVD of each edge probability block $P^{(kl)}$ to avoid the unidentifiable multiplicative constants.

$$\text{RMSE}(\{\hat{\lambda}^{(kl)}\}_K, \{\lambda^{(kl)}\}_K) = \sqrt{\frac{1}{n} \sum_{k < l} \min_{s=\pm 1} \|s\hat{\lambda}^{(kl)} - \lambda^{(kl)}\|_2^2}$$

We can also avoid the unidentifiable multiplicative constant more directly by reconstructing each $\hat{P}^{(kl)} = \hat{\lambda}^{(kl)}(\hat{\lambda}^{(lk)})^\top$, which we use to define another parameter estimation error.

$$\text{RMSE}(\hat{P}, P) = \sum_{k,l} \sqrt{\frac{1}{n_k n_l} \|P^{(kl)} - \hat{P}^{(kl)}\|_F^2}$$

4.1 Balanced communities

In each simulation, community labels z_1, \dots, z_n were drawn from a multinomial distribution with mixture parameters $\{\alpha_1, \dots, \alpha_K\}$, then $\{\lambda^{(kl)}\}_K$ according to the drawn community labels, P was constructed using the drawn $\{\lambda^{(kl)}\}_K$, and A was drawn from P by $A_{ij} \overset{\text{indep}}{\sim} \text{Bernoulli}(P_{ij})$. Each simulation has a unique edge probability matrix P .

For these examples, we set the following parameters:

- Number of vertices $n = 128, 256, 512, 1024, 2048, 4096$
- Number of underlying communities $K = 2, 3, 4$
- Mixture parameters $\alpha_k = 1/K$ for $k = 1, \dots, K$, (i.e., each community label has an equal probability of being drawn)
- Community labels $z_k \stackrel{\text{iid}}{\sim} \text{Multinomial}(\alpha_1, \dots, \alpha_K)$
- Within-group popularities $\lambda^{(kk)} \stackrel{\text{iid}}{\sim} \text{Beta}(2, 1)$
- Between-group popularities $\lambda^{(kl)} \stackrel{\text{iid}}{\sim} \text{Beta}(1, 2)$ for $k \neq l$

50 simulations were performed for each (n, K) pair.

Fig 1 shows OSC’s community detection error going to 0 for large n . SSC on both the embedding and on the adjacency matrix produces similar results for $K > 2$. Weaker performance of SSC for $K = 2$ can be attributed to the final spectral clustering step of the affinity matrix. A GMM was fit to the Laplacian eigenmap, but visual inspection suggests that the communities are not distributed as a mixture of Gaussians in the eigenmap. While the subspace detection property is guaranteed for large n , in our simulations, setting a large enough sparsity parameter for SSC resulted in more than K disconnected subgraphs.

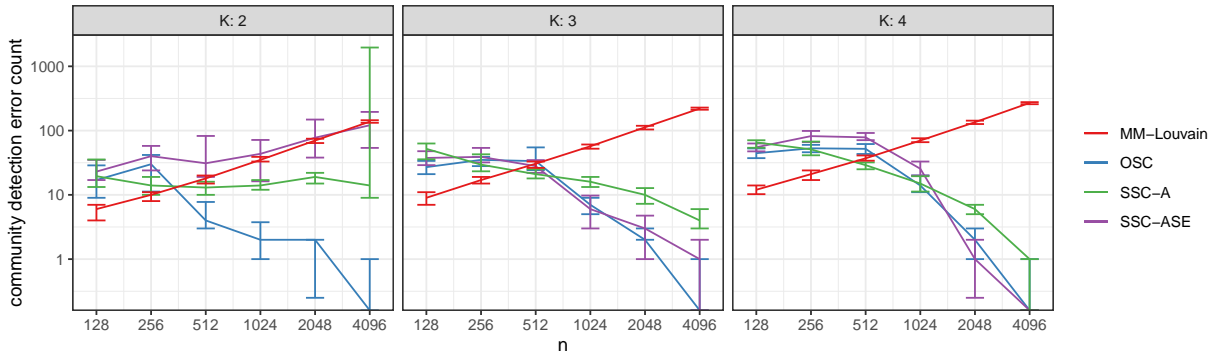


Figure 1: Median and IQR of community detection error. Communities are approximately balanced. Simulations were repeated 50 times for each sample size.

Given ground truth community labels, Algorithm 3 and the MLE-based plug-in estimators [15] perform similarly, with root mean square error decaying at rate approximately $n^{-1/2}$.

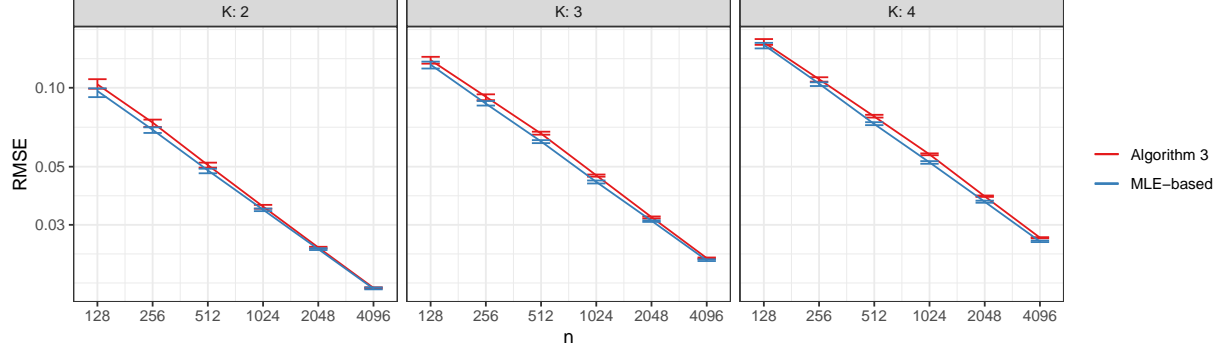


Figure 2: Median and IQR RMSE from Algorithm 3 (red) compared against an MLE-based method (blue). Simulations were repeated 50 times for each sample size. Communities were drawn to be approximately balanced.

4.2 Imbalanced communities

Simulations performed in this section are similar to those in the previous section with the exception of the mixture parameters $\{\alpha_1, \dots, \alpha_K\}$ used to draw community labels from the multinomial distribution. For these examples, we set the following parameters:

- Number of vertices $n = 128, 256, 512, 1024, 2048, 4096$
- Number of underlying communities $K = 2, 3, 4$
- Mixture parameters $\alpha_k = \frac{k^{-1}}{\sum_{l=1}^K l^{-1}}$ for $k = 1, \dots, K$
- Community labels $z_k \stackrel{\text{iid}}{\sim} \text{Multinomial}(\alpha_1, \dots, \alpha_K)$
- Within-group popularities $\lambda^{(kk)} \stackrel{\text{iid}}{\sim} \text{Beta}(2, 1)$
- Between-group popularities $\lambda^{(kl)} \stackrel{\text{iid}}{\sim} \text{Beta}(1, 2)$ for $k \neq l$

50 simulations were performed for each (n, K) pair.

We again see community detection error trending to 0 for OSC, as well as for SSC when $K > 2$ (Fig. 3). Alg. 3 continues to see $n^{-1/2}$ decay in parameter estimation error (4).

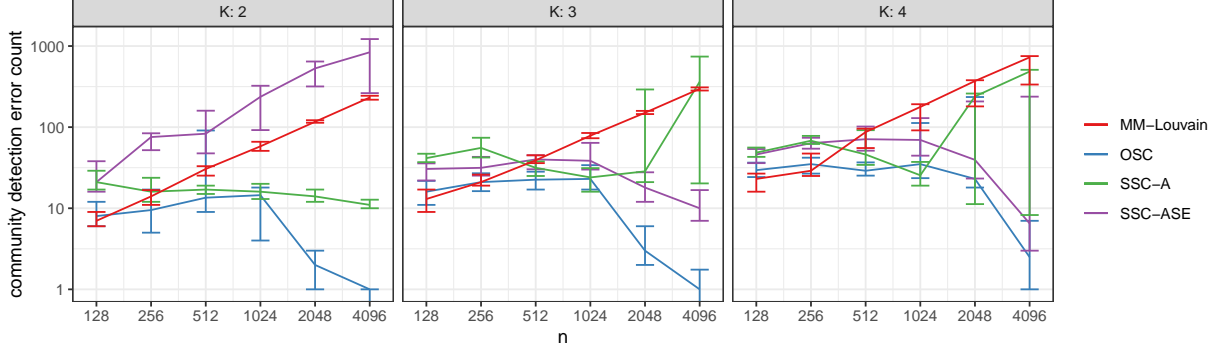


Figure 3: Median and IQR of community detection error. Communities are imbalanced. Simulations were repeated 50 times for each sample size.

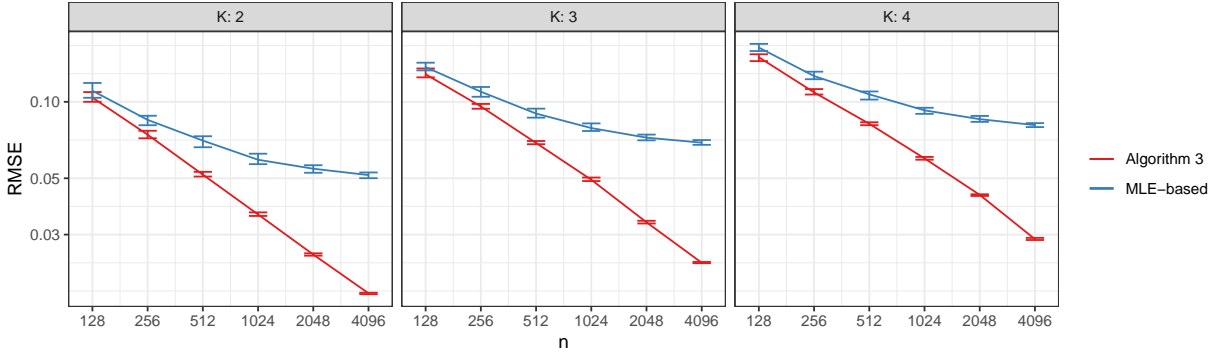


Figure 4: Median and IQR RMSE from Algorithm 3 (red) compared against an MLE-based method (blue). Simulations were repeated 50 times for each sample size. Communities were drawn to be imbalanced.

5 Real data examples

In the first real data example, we applied OSC to the Leeds Butterfly dataset [18] consisting of visual similarity measurements among 832 butterflies across 10 species. The graph was modified to match the example from Noroozi et al.: Only the 4 most frequent species were considered, and the similarities were discretized to $\{0, 1\}$ via thresholding. Fig. 5 shows a sorted adjacency matrix sorted by the resultant clustering.

Comparing against the ground truth species labels, OSC achieves an accuracy of 63% and

Table 1: Community detection error rates for modularity maximization, sparse subspace clustering, and OSC.

Network	MM	SSC-ASE	OSC
British MPs	0.003	0.018	0.009
Political blogs	0.050	0.196	0.062
DBLP	0.028	0.087	0.059

an adjusted Rand index of 73%. In comparison, [Noroozi et al.](#) achieved an adjusted Rand index of 73% using sparse subspace clustering on the same dataset.

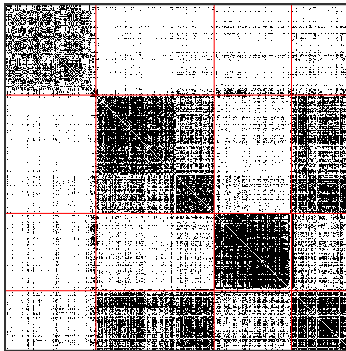


Figure 5: Adjacency matrix of the Leeds Butterfly dataset after sorting by the clustering outputted by OSC.

In the second example, we applied OSC to the British MPs Twitter network [5], the Political Blogs network [1], and the DBLP network [4] [6]. For this data analysis, we subsetting the data as described by [Sengupta and Chen](#) for their analysis of the same networks. Our methods underperformed compared to modularity maximization, although performance is comparable. In addition, OSC’s runtime is much lower than that of modularity maximization.

Table 2: Community detection error rates for identifying household religion.

Network	MM	SSC-ASE	OSC
Village 12	0.270	0.291	0.227
Village 31	0.125	0.066	0.110
Village 46	0.052	0.463	0.078

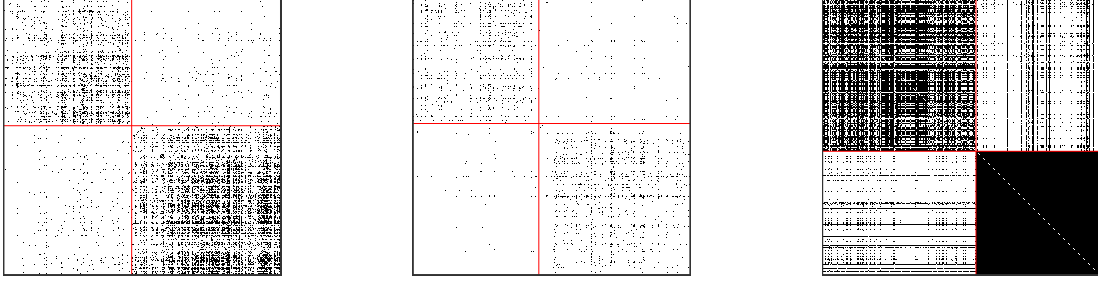


Figure 6: Adjacency matrices of (from left to right) the British MPs, Political Blogs, and DBLP networks after sorting by the clustering outputted by OSC.

In the third example, we consider the Karnataka villages data studied by Banerjee et al. [2]. For this example, we chose the `visitgo` networks from villages 12, 31, and 46 at the household level. The label of interest is the religious affiliation. The networks were truncated to religions “1” and “2”, and vertices of degree 0 were removed.

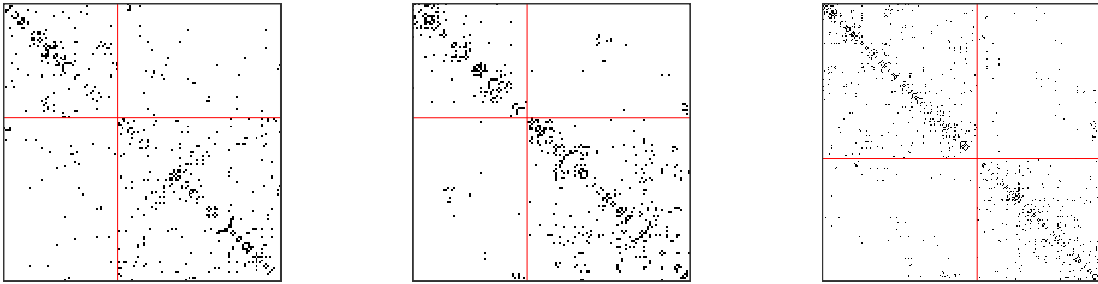


Figure 7: Adjacency matrix of the Karnataka villages data, arranged by the clustering produced by OSC (left). The villages studied here are, from left to right, 12, 31, and 46.

6 Discussion

This paper shows the connection between the PABM and the GRDPG, namely that a PABM graph can be represented as a union of orthogonal subspaces in an embedding under the GRDPG framework. We then exploited this relationship to develop community detection and parameter estimation methods. In fact, we can represent any graph with Bernoulli edges as a GRDPG, and in the PABM case, it turns out that this relationship leads to a very straightforward applications of previous work from [Rubin-Delanchy et al.](#), [Soltanolkotabi and Candés](#), and [Wang and Xu](#), which lead to asymptotically correct solutions with high probability. Similar methods can be applied for other models, such as the Nested Block Model [\[11\]](#).

7 Proofs

Proof of Theorem 1. This is given by straightforward matrix multiplication. It suffices to show that

$$XUI_{3,1}U^\top X^\top = \begin{bmatrix} \lambda^{(11)}(\lambda^{(11)})^\top & \lambda^{(12)}(\lambda^{(21)})^\top \\ \lambda^{(21)}(\lambda^{(12)})^\top & \lambda^{(22)}(\lambda^{(22)})^\top \end{bmatrix}$$

Remark. While we can just perform the matrix multiplication to show the equivalence, it is more illustrative to look at a few intermediate steps. Note that the product of the three inner matrices results in a permutation matrix with fixed points at positions 1 and 4 and a cycle of order 2 swapping positions 2 and 3:

$$UI_{3,1}U^\top = \begin{bmatrix} 1 & 0 & 0 & 0 \\ 0 & 0 & 1 & 0 \\ 0 & 1 & 0 & 0 \\ 0 & 0 & 0 & 1 \end{bmatrix} = \Pi$$

Since U is orthonormal and $I_{3,1}$ is diagonal, $\Pi = UI_{3,1}U^\top$ is a spectral decomposition

of this permutation matrix. Note that the two fixed points result in eigenvalues of $+1$ with corresponding eigenvectors e_i where $i = 1, 4$ corresponding to the locations of the fixed points, and the cycle of order two results in two eigenvalues ± 1 with corresponding eigenvectors $(e_i \pm e_j)/\sqrt{2}$ where $i = 2, j = 3$, pair that is swapped.

Lemma 1. *Let $P = VDV^\top$ be the spectral decomposition of the edge probability matrix for a PABM. Then $VV^\top = X(X^\top X)^{-1}X^\top$ where X is defined as in (3).*

Proof. By Theorem 2, $P = XU I_{p,q} U^\top X^\top$, where X is defined as in (3) and $p = K(K+1)/2$ and $q = K(K-1)/2$. Alternatively, the spectral decomposition can be written as $P = VDV^\top = V|D|^{1/2} I_{p,q} |D|^{1/2} V^\top$ for the same (p, q) and $|\cdot|^{1/2}$ is applied entry-wise. Thus for some $Q \in \mathbb{O}(p, q)$,

$$XUQ = V|D|^{1/2}$$

Therefore, using the fact that $UU^\top = I$ and $V^\top V = I$,

$$(V|D|^{1/2})((V|D|^{1/2})^\top(V|D|^{1/2}))^{-1}(V|D|^{1/2})^\top = (XUQ)((XUQ)^\top(XUQ))^{-1}(XUQ)^\top$$

The right-hand side becomes

$$\begin{aligned} (XUQ)((XUQ)^\top(XUQ))^{-1}(XUQ)^\top &= XUQQ^{-1}U^\top(X^\top X)^{-1}U(Q^\top)^{-1}Q^\top U^\top X^\top \\ &= XU U^\top (X^\top X)^{-1}U U^\top X^\top \\ &= X(X^\top X)^{-1}X^\top \end{aligned}$$

The left-hand side becomes:

$$\begin{aligned} (V|D|^{1/2})((V|D|^{1/2})^\top(V|D|^{1/2}))^{-1}(V|D|^{1/2})^\top &= V|D|^{1/2}|D|^{-1/2}(V^\top V)^{-1}|D|^{-1/2}|D|^{1/2}V^\top \\ &= VV^\top \end{aligned}$$

Proof of Theorem 3. By Lemma 1, $VV^\top = X(X^\top X)^{-1}X^\top$ where X is defined as in (3). Since X is block diagonal with each block corresponding to one community, $X(X^\top X)^{-1}X^\top$ is also a block diagonal matrix with each block corresponding to a community and zeros elsewhere. Therefore, if vertices i and j belong to different communities, then the ij^{th} element of $nX(X^\top X)^{-1}X^\top = nVV^\top = B$ is 0.

Proof of Theorem 4. Let V_n and \hat{V}_n be the eigenvectors of P and A corresponding to the $K(K+1)/2$ most positive and $K(K-1)/2$ most negative eigenvalues. By Rubin-Delanchy et al., for some $W \in \mathbb{O}(K^2)$, and $c > 0$,
 $\|\hat{V}W - V\|_{2 \rightarrow \infty} = O_P\left(\frac{(\log n)^c}{n\sqrt{\rho_n}}\right)$. We furthermore have $\|V\|_{2 \rightarrow \infty} = O_P(n^{-1/2})$. Then if $(v_n^{(i)})^\top$ and $(\hat{v}_n^{(i)})^\top$ correspond to the rows of V_n and \hat{V}_n , for i and j in different communities, using the fact that $(v_n^{(i)})^\top v_n^{(j)} = 0$,

$$\begin{aligned}
\max_{i,j} |(\hat{v}_n^{(i)})^\top \hat{v}_n^{(j)}| &= \max_{i,j} |(\hat{v}_n^{(i)})^\top \hat{v}_n^{(j)} - (v_n^{(i)})^\top v_n^{(j)}| \\
&= \max_{i,j} |(\hat{v}_n^{(i)})^\top WW^\top \hat{v}_n^{(j)} - (v_n^{(i)})^\top v_n^{(j)}| \\
&= \|\hat{V}_n W^\top W \hat{V}_n - V_n V_n^\top\|_{2 \rightarrow \infty} \\
&= \|2\hat{V}_n W V_n^\top - 2V_n V_n^\top + \hat{V}_n W W^\top \hat{V}_n^\top - 2\hat{V}_n W V_n^\top + V_n V_n^\top\|_{2 \rightarrow \infty} \\
&= \|2(\hat{V}_n W - V_n)V_n^\top + (\hat{V}_n W - V_n)(\hat{V}_n W - V_n)^\top\|_{2 \rightarrow \infty} \\
&\leq 2\|\hat{V}_n W - V_n\|_{2 \rightarrow \infty}\|V_n\|_{2 \rightarrow \infty} + \|\hat{V}_n W - V_n\|_{2 \rightarrow \infty}^2 \\
&= O_P\left(\frac{(\log n)^c}{n^{3/2}\rho_n^{1/2}}\right)
\end{aligned}$$

Then scaling by n , we get $|n(\hat{v}_n^{(i)})^\top \hat{v}_n^{(j)}| = O_P\left(\frac{(\log n)^c}{\sqrt{n\rho_n}}\right)$.

Definition 5 (Inradius [16, 19]). *The inradius of a convex body \mathcal{P} , denoted by $r(\mathcal{P})$, is defined as the radius of the largest Euclidean ball inscribed in \mathcal{P} . In addition, $r(X)$ for data matrix X with rows x_i^\top represents the inradius of the symmetric convex hull of X .*

Definition 6 (Subspace incoherence property [19]).

Lemma 2. *Let \hat{V} be the eigenvectors of A_n corresponding to the $K(K+1)/2$ most positive and $K(K-1)/2$ most negative eigenvalues such that the rows of \hat{V} are ordered by community,*

and let $\hat{V}^{(k)}$ be the rows of the k^{th} community in \hat{V} and $\hat{V}^{(-k)}$ be the rows of \hat{V} with the k^{th} community omitted. Denote $(\hat{v}_i^{(k)})^\top$ as the rows of \hat{V} , $\hat{V}_{-i}^{(k)}$ as $\hat{V}^{(k)}$ with the i^{th} row omitted, and $\mathcal{S}^{(k)}$ as the subspace spanned by $V^{(k)}$. Let V , $V^{(k)}$, $V^{(-k)}$, and $v_i^{(k)}$ be the corresponding values for P_n .

Let $\nu_i^{(k)} = \max_{\eta} (\hat{v}_i^{(k)})^\top \eta - \frac{1}{2\lambda} \eta^\top \eta$ subject to $\|V_{-i}^{(k)} \eta\|_\infty \leq 1$, and define the projected dual direction $w_i^{(k)}$ as $\mathbb{P}_{\mathcal{S}^{(k)}}(\nu_i^{(k)})$ normalized to length 1. Collect the projected dual directions into $W = \begin{bmatrix} w_1^{(k)} & \dots & w_{n_k}^{(k)} \end{bmatrix}^\top$.

Define the subspace incoherence:

$$\mu_n^{(k)} = \mu(\hat{V}^{(k)}) = \max_{v \in V^{(-k)}} \|W^{(k)} v\|_\infty$$

Then $\forall k, n$,

$$\mu_n^{(k)} = 0 \tag{10}$$

Proof. Since by Theorem 2 each $\mathcal{S}^{(k)}$ are mutually orthogonal, any vector projected to $\mathcal{S}^{(k)}$ must be orthogonal to each row of $V^{(-k)}$. Therefore, $W^{(k)} v = 0 \forall v \in \mathcal{S}^{(-k)}$.

Lemma 3. Let $(v_n^{(i)})^\top$ and $(\hat{v}_n^{(i)})^\top$ be the rows of V_n and \hat{V}_n respectively. By [Rubin-Delanchy et al.](#),

$$\delta_n = \max_i \|\hat{v}_n^{(i)} - v_n^{(i)}\| \xrightarrow{\text{a.s.}} 0 \tag{11}$$

Proof of Theorem 5. The basis of this proof is Theorem 6 from [Wang and Xu](#), which states that the subspace detection property holds if the noise is small enough and the subspace inradius is greater than the subspace incoherence for each community k .

Let $V_{n,-i}^{(k)}$ be $V_n^{(k)}$ with the i^{th} entry removed. Suppose that for each community k , there are enough vertices such that for each i , $V_{n,-i}^{(k)}$ spans its corresponding subspace (Theorem 2).

Then $r_n^{(k)} = \min_i r(V_{n,-i}^{(k)}) > 0$. Thus by (10), for each k , $r_n^{(k)} > \mu_n^{(k)} = 0$ where $\mu_n^{(k)} = \mu(\hat{V}_n^{(k)})$ and n is large enough such that $\min_{k,i} \text{rank}(V_{n,-i}^{(k)}) = K$.

Let $r_n = \min_k r_n^{(k)}$. By (11), $\delta_n \xrightarrow{a.s.} 0$. Then as $n \rightarrow \infty$, $\delta_n < \min_k \frac{r_n(r_n^{(k)} - \mu_n^{(k)})}{2 + 7r_n^{(k)}} = \min_k \frac{r_n r_n^{(k)}}{2 + 7r_n^{(k)}}$ with probability 1.

Thus the conditions for the subspace detection property from Theorem 6 from Wang and Xu are satisfied with probability 1 as $n \rightarrow \infty$.

Remark. Theorem 6 of Wang and Xu assume that each $\|v_n^{(i)}\| = 1$, which scales each $r_n^{(k)} \leq 1$. This is not strictly necessary for the proof of Theorem 5 since each $\mu_n^{(k)} = 0$, so as long as the k^{th} community spans its subspace, $ar_n^{(k)} > 0 = \mu_n^{(k)} \forall a > 0$.

Proof of Theorem 6. Let P and A be organized by community such that the elements of blocks $P^{(kl)}$ and $A^{(kl)}$ correspond to the edges between communities k and l .

Case $k = l$. $P^{(kk)}$ and $A^{(kk)}$ represent within-community edge probabilities and edges for community k .

By definition, $P^{(kk)} = \lambda^{(kk)}(\lambda^{(kk)})^\top$. This implies that the singular value decomposition $P^{(kk)} = \sigma_{kk}^2 u^{(kk)}(u^{(kk)})^\top$ has one singular value and one pair of singular vectors ($P^{(kk)}$ is symmetric, so the left and right singular vectors are identical). Then $\lambda^{(kk)} = \sigma_{kk} u^{(kk)}$.

Let $\hat{U}^{(kk)} \hat{\Sigma}^{(kk)} (\hat{U}^{(kk)})^\top$ be the singular value decomposition of $A^{(kk)}$, and let $\hat{\sigma}_{kk}^2 \hat{u}^{(kk)} (\hat{u}^{(kk)})^\top$ be its one-dimensional approximation. Define $\hat{\lambda}^{(kk)} = \hat{\sigma}_{kk} \hat{u}^{(kk)}$. Then $\hat{\lambda}^{(kk)}$ is the adjacency spectral embedding approximation of $\lambda^{(kk)}$.

Then by Theorem 5 of Rubin-Delanchy et al., the adjacency spectral embedding $\hat{\lambda}^{(kk)}$ approximates $\lambda^{(kk)}$ at rate $\frac{(\log n_k)^c}{\sqrt{n_k}}$.

Case $k \neq l$. $P^{(kl)}$ and $A^{(kl)}$ represent edge probabilities and edges between communities k and l . Note that $P^{(kl)} = (P^{(lk)})^\top$.

By definition, $P^{(kl)} = \lambda^{(kl)}(\lambda^{(lk)})^\top$. As in the $k = l$ case, we note that the singular value decomposition $P^{(kl)} = \sigma_{kl}^2 u^{(kl)}(v^{(kl)})^\top$ is one-dimensional and $\lambda^{(kl)} = \sigma_{kl} u^{(kl)}$. (We can also note that the SVD of $P^{(lk)} = \sigma_{kl}^2 v^{(kl)}(u^{(kl)})^\top$, i.e., $\sigma_{kl} = \sigma_{lk}$, $u^{(kl)} = v^{(lk)}$, and $v^{(kl)} = u^{(lk)}$.)

Now consider the Hermitian dilation

$$M^{(kl)} = 2 \begin{bmatrix} 0 & P^{(kl)} \\ P^{(lk)} & 0 \end{bmatrix}$$

which is a symmetric $(n_k + n_l) \times (n_k + n_l)$ matrix. It can be shown that the spectral decomposition of $M^{(kl)}$ is

$$M^{(kl)} = \begin{bmatrix} u^{(kl)} & -u^{(kl)} \\ v^{(kl)} & v^{(kl)} \end{bmatrix} \times \begin{bmatrix} \sigma_{kl}^2 & 0 \\ 0 & -\sigma_{kl}^2 \end{bmatrix} \times \begin{bmatrix} u^{(kl)} & -u^{(kl)} \\ v^{(kl)} & v^{(kl)} \end{bmatrix}^\top$$

Thus treating $M^{(kl)}$ as the edge probability matrix of a GRDPG, we have latent positions in \mathbb{R}^2 given by

$$\begin{bmatrix} \sigma_{kl} u^{(kl)} & \sigma_{kl} u^{(kl)} \\ \sigma_{kl} v^{(kl)} & -\sigma_{kl} v^{(kl)} \end{bmatrix} = \begin{bmatrix} \lambda^{(kl)} & \lambda^{(kl)} \\ \lambda^{(lk)} & -\lambda^{(lk)} \end{bmatrix}$$

Now consider

$$\hat{M}^{(kl)} = \begin{bmatrix} 0 & A^{(kl)} \\ A^{(lk)} & 0 \end{bmatrix}$$

Then $\hat{M}^{(kl)} = M^{(kl)} + E'$ where

$$E' = \begin{bmatrix} 0 & E \\ E^\top & 0 \end{bmatrix}$$

and E is the $n_k \times n_l$ matrix of independent noise (to generate the Bernoulli entries in $A^{(kl)}$). Then $\hat{M}^{(kl)}$ is an adjacency matrix drawn from $M^{(kl)}$, so its adjacency spectral embedding, given by

$$\begin{bmatrix} \hat{\lambda}^{(kl)} & \hat{\lambda}^{(kl)} \\ \hat{\lambda}^{(lk)} & -\hat{\lambda}^{(lk)} \end{bmatrix}$$

where each $\hat{\lambda}^{(kl)}$ is defined as in Algorithm 3, approximates the latent positions of $M^{(kl)}$ up to indefinite orthogonal transformation by the rate given in Theorem 5 of [Rubin-Delanchy et al.](#).

In this case, the indefinite orthogonal transformation W_* in the GRDPG result [13] is of the form $U^\top \hat{U}$. The eigenvalues of M are distinct since the signature for this GRDPG is $(1, 1)$, and $U^\top \hat{U}$ is block diagonal, resulting in $W_* \xrightarrow{a.s.} I$. Therefore, the adjacency spectral embedding of $\hat{M}^{(kl)}$ is a direct estimation of the specific latent positions outlined for $M^{(kl)}$, up to sign flip.

References

- [1] Lada A. Adamic and Natalie Glance. The political blogosphere and the 2004 u.s. election: Divided they blog. In *Proceedings of the 3rd International Workshop on Link Discovery*, LinkKDD '05, page 36–43, New York, NY, USA, 2005. Association for Computing Machinery. ISBN 1595932151. doi: 10.1145/1134271.1134277. URL <https://doi.org/10.1145/1134271.1134277>.
- [2] Abhijit Banerjee, Arun G. Chandrasekhar, Esther Duflo, and Matthew O. Jackson. The Diffusion of Microfinance, 2013. URL <https://doi.org/10.7910/DVN/U3BIHX>.
- [3] Gabor Csardi and Tamas Nepusz. The igraph software package for complex network research. *InterJournal*, Complex Systems:1695, 2006. URL <https://igraph.org>.
- [4] Jing Gao, Feng Liang, Wei Fan, Yizhou Sun, and Jiawei Han. Graph-based consensus maximization among multiple supervised and unsupervised models. In Y. Bengio, D. Schuurmans, J. D. Lafferty, C. K. I. Williams, and A. Culotta, editors, *Advances in Neural Information Processing Systems 22*, pages 585–593. Curran Associates, Inc., 2009. URL <http://papers.nips.cc/paper/3855-graph-based-consensus-maximization-among-multiple-supervised-and-unsupervised-models.pdf>.
- [5] Derek Greene and Pádraig Cunningham. Producing a unified graph representation from multiple social network views. *CoRR*, abs/1301.5809, 2013. URL <http://arxiv.org/abs/1301.5809>.

- [6] Ming Ji, Yizhou Sun, Marina Danilevsky, Jiawei Han, and Jing Gao. Graph regularized transductive classification on heterogeneous information networks. In José Luis Balcázar, Francesco Bonchi, Aristides Gionis, and Michèle Sebag, editors, *Machine Learning and Knowledge Discovery in Databases*, pages 570–586, Berlin, Heidelberg, 2010. Springer Berlin Heidelberg. ISBN 978-3-642-15880-3.
- [7] Brian Karrer and M. E. J. Newman. Stochastic blockmodels and community structure in networks. *Physical Review E*, 83(1), Jan 2011. ISSN 1550-2376. doi: 10.1103/PhysRevE.83.016107. URL <http://dx.doi.org/10.1103/PhysRevE.83.016107>.
- [8] Can M. Le, Elizaveta Levina, and Roman Vershynin. Optimization via low-rank approximation for community detection in networks. *Ann. Statist.*, 44(1):373–400, 02 2016. doi: 10.1214/15-AOS1360. URL <https://doi.org/10.1214/15-AOS1360>.
- [9] François Lorrain and Harrison C. White. Structural equivalence of individuals in social networks. *The Journal of Mathematical Sociology*, 1(1):49–80, 1971. doi: 10.1080/0022250X.1971.9989788. URL <https://doi.org/10.1080/0022250X.1971.9989788>.
- [10] Vince Lyzinski, Daniel L. Sussman, Minh Tang, Avanti Athreya, and Carey E. Priebe. Perfect clustering for stochastic blockmodel graphs via adjacency spectral embedding. *Electron. J. Statist.*, 8(2):2905–2922, 2014. doi: 10.1214/14-EJS978. URL <https://doi.org/10.1214/14-EJS978>.
- [11] Majid Noroozi and Marianna Pensky. The hierarchy of block models, 2021.
- [12] Majid Noroozi, Ramchandra Rimal, and Marianna Pensky. Estimation and clustering in popularity adjusted block model. *Journal of the Royal Statistical Society: Series B (Statistical Methodology)*, n/a(n/a), 2021+. doi: <https://doi.org/10.1111/rssb.12410>. URL <https://rss.onlinelibrary.wiley.com/doi/abs/10.1111/rssb.12410>.
- [13] Patrick Rubin-Delanchy, Joshua Cape, Minh Tang, and Carey E. Priebe. A statistical interpretation of spectral embedding: the generalised random dot product graph, 2017.
- [14] Patrick Rubin-Delanchy, Carey E. Priebe, and Minh Tang. Consistency of adjacency spectral embedding for the mixed membership stochastic blockmodel, 2017.

- [15] Srijan Sengupta and Yuguo Chen. A block model for node popularity in networks with community structure. *Journal of the Royal Statistical Society. Series B: Statistical Methodology*, 80(2):365–386, March 2018. ISSN 1369-7412. doi: 10.1111/rssb.12245.
- [16] Mahdi Soltanolkotabi and Emmanuel J. Candès. A geometric analysis of subspace clustering with outliers. *Ann. Statist.*, 40(4):2195–2238, 08 2012. doi: 10.1214/12-AOS1034. URL <https://doi.org/10.1214/12-AOS1034>.
- [17] Mahdi Soltanolkotabi, Ehsan Elhamifar, and Emmanuel J. Candès. Robust subspace clustering. *Ann. Statist.*, 42(2):669–699, 04 2014. doi: 10.1214/13-AOS1199. URL <https://doi.org/10.1214/13-AOS1199>.
- [18] Bo Wang, Armin Pourshafeie, Marinka Zitnik, Junjie Zhu, Carlos D. Bustamante, Serafim Batzoglou, and Jure Leskovec. Network enhancement as a general method to denoise weighted biological networks. *Nature Communications*, 9(1), Aug 2018. ISSN 2041-1723. doi: 10.1038/s41467-018-05469-x. URL <http://dx.doi.org/10.1038/s41467-018-05469-x>.
- [19] Yu-Xiang Wang and Huan Xu. Noisy sparse subspace clustering. *Journal of Machine Learning Research*, 17(12):1–41, 2016. URL <http://jmlr.org/papers/v17/13-354.html>.
- [20] Stephen J. Young and Edward R. Scheinerman. Random dot product graph models for social networks. In Anthony Bonato and Fan R. K. Chung, editors, *Algorithms and Models for the Web-Graph*, pages 138–149, Berlin, Heidelberg, 2007. Springer Berlin Heidelberg. ISBN 978-3-540-77004-6.